



# Active metal template synthesis of a neutral indolocarbazole-containing [2]rotaxane host system for selective oxoanion recognition

Received 00th January 20xx,  
Accepted 00th January 20xx

DOI: 10.1039/x0xx00000x

www.rsc.org/

Asha Brown,<sup>a</sup> Thomas Lang,<sup>a</sup> Kathleen M. Mullen<sup>a</sup> and Paul D. Beer<sup>a\*</sup>

An active metal template strategy was used to synthesise a neutral indolocarbazole containing [2]rotaxane anion host system. <sup>1</sup>H NMR anion binding investigations reveal that the [2]rotaxane recognises a range of monoanions in acetone-d<sub>5</sub>:D<sub>2</sub>O 95:5 with an unusual interlocked host selectivity for acetate and dihydrogenphosphate oxoanions over halides. The rotaxane displays an overall selectivity for the sulfate dianion, favouring a 2:1 host:guest binding stoichiometry at low sulfate concentration and a 1:1 stoichiometry in the presence of excess sulfate. Fluorescence titration demonstrate that the [2]rotaxane is also capable of sensing guest anions via significant changes in its emission spectrum.

## Introduction

Mechanically interlocked rotaxane and catenane molecules were recently heralded as key components in a new era of *molecular robotics*<sup>1,2</sup> and the exploration of controlled molecular motion in these systems is a topical theme within supramolecular chemistry.<sup>3</sup> In parallel, increasing attention is being devoted to the exploration of the host–guest chemistry of interlocked rotaxane and catenane molecules owing to their potential to incorporate internal preorganised, three-dimensional binding pockets which can effectively shield an encapsulated guest species from the bulk solvent medium. Since anionic substrates exhibit a range of three-dimensional geometries and high solvation enthalpies in protic solvents, interlocked molecules are particularly attractive as potential host systems for anions. Emulating Sauvage's classical passive metal template approach,<sup>4,5</sup> we have used anions as discrete templates to direct the assembly of interlocked rotaxane and catenane host systems. Upon removal of the template, the interlocked product contains a cavity which is complementary in size and shape to the anion which directed its formation. Using this methodology we have developed a variety of rotaxane- and catenane-based anion receptors which selectively bind various anions in competitive solvent media.<sup>6,7</sup> However, there remain some instances when the use of anion templation fails to yield the desired interlocked product. For example, while the heterocyclic indolo-[2,3a]-carbazole group – a potent bidentate hydrogen-bond-donor motif with integral

fluorescent anion sensing capability<sup>8</sup> – has been elegantly incorporated into macrocyclic<sup>9–12</sup> and foldameric<sup>13–18</sup> anion receptors, along with two structurally related homocatenane receptors,<sup>19,20</sup> the anion-templated synthesis of an indolocarbazole-containing [2]rotaxane anion receptor is yet to be achieved. Although sulfate and fluoride anions were shown to template the orthogonal interpenetrative assembly of an indolocarbazole threading component and isophthalamide-containing macrocycle,<sup>21</sup> this anion templated pseudorotaxane assembly process has not to date been successfully extended to the synthesis of a permanently interlocked rotaxane species in the solution phase.<sup>22</sup> The single reported example of an indolocarbazole [2]rotaxane relied on an alternative template approach which exploited favourable charge-transfer and electrostatic interactions between an electron-rich indolocarbazole threading component and electron-deficient tetracationic 4,4-bipyridinium macrocycle component; however the inherent instability of the dicationic 4,4-bipyridinium motif towards oxoanions precluded a full investigation of the anion recognition properties of this receptor.<sup>23</sup>

During the last decade the active metal template strategy<sup>24</sup> has emerged as an efficient approach to the construction of interlocked molecules which has rapidly grown in scope and popularity. In particular, the copper(I)-catalysed azide-alkyne cycloaddition (CuAAC) variant<sup>25,26</sup> has been elegantly exploited in the synthesis of a fascinating range of rotaxane, catenane and knot molecules.<sup>27–34</sup> Herein we describe the use of a CuAAC reaction in the active metal template synthesis of a previously inaccessible neutral indolocarbazole [2]rotaxane anion host system. <sup>1</sup>H NMR anion binding investigations reveal that the rotaxane host recognises a range of monoanions in acetone-d<sub>5</sub>:D<sub>2</sub>O 95:5 with a preference for oxoanions over halides, which is unusual and rare among interlocked anion receptors.<sup>35</sup> Strong and selective binding of the sulfate dianion

<sup>a</sup> Chemistry Research Laboratory, Department of Chemistry, University of Oxford, Mansfield Road, Oxford, UK, OX1 3TA. E-mail: paul.beer@chem.ox.ac.uk  
Electronic Supplementary Information (ESI) available: synthetic procedures and characterisation data, <sup>1</sup>H NMR and <sup>13</sup>C NMR spectra of all new compounds, <sup>1</sup>H NMR and fluorescence titration protocols, spectra and binding curves.  
See DOI: 10.1039/x0xx00000x

is also demonstrated, and the [2]rotaxane is shown to be capable of sensing anions via changes in its fluorescence emission spectrum.

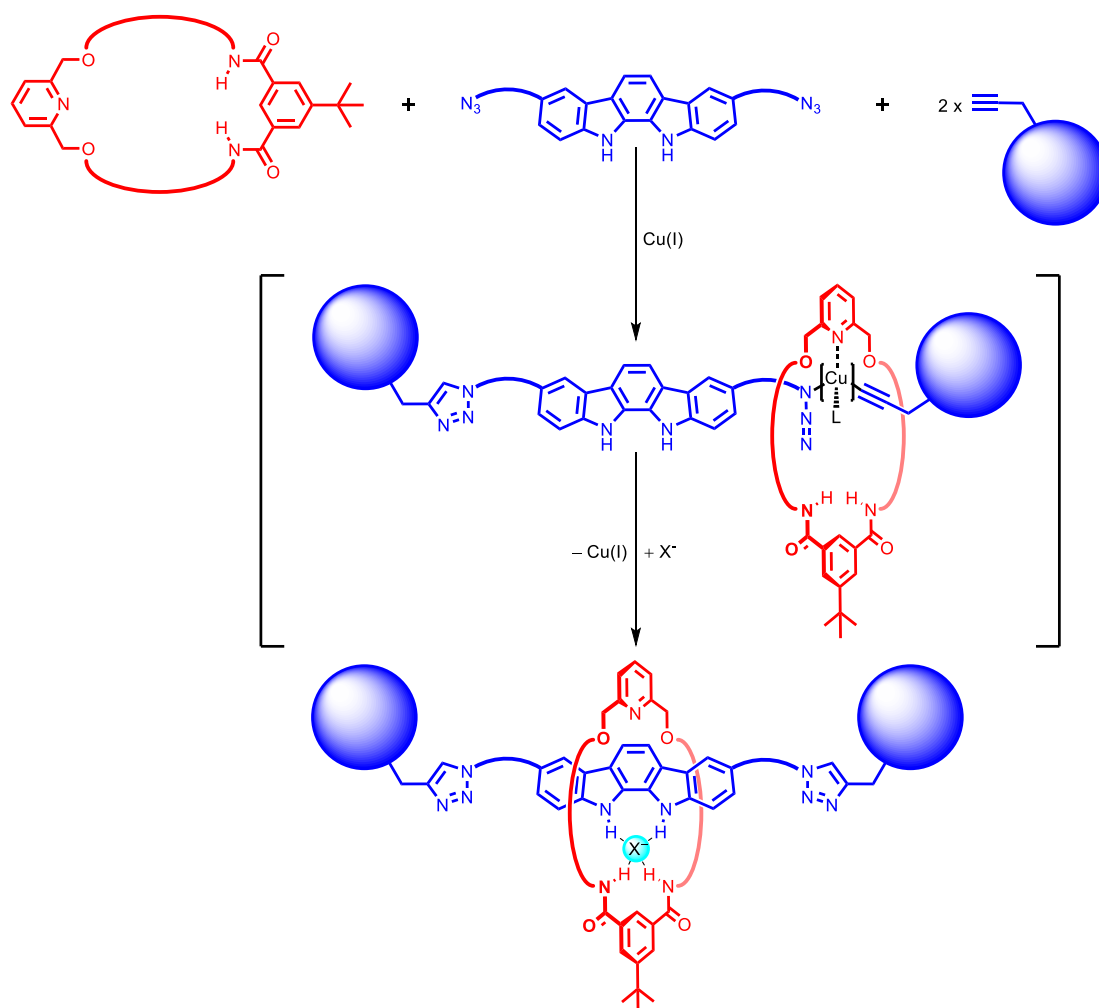
## Results and discussion

### Design and synthesis of the indolocarbazole [2]rotaxane host

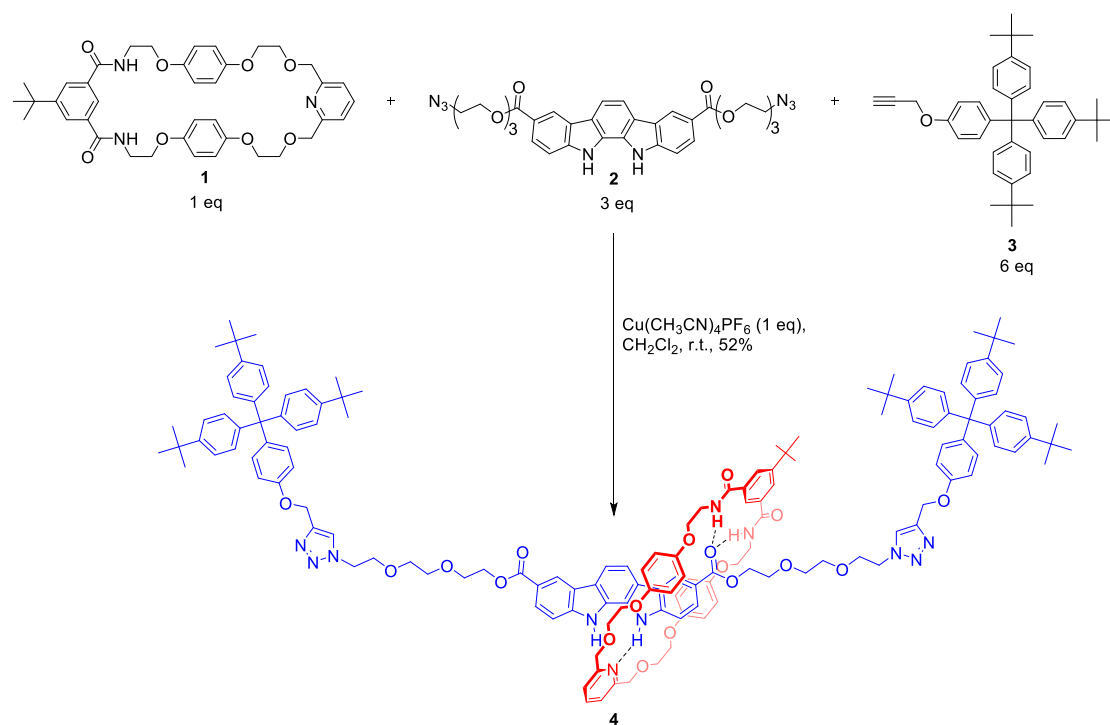
The design and active metal template approach to the synthesis of the target indolocarbazole [2]rotaxane anion host system is illustrated in Scheme 1. The rotaxane incorporates bidentate indolocarbazole and isophthalamide hydrogen-bond-donor motifs in the axle and macrocycle components respectively, which are designed to convergently bind to a guest anion within a pseudotetrahedral interlocked binding pocket. Taking inspiration from Leigh and co-workers' elegant work on the development of the original CuAAC active metal template rotaxane synthesis methodology,<sup>25,26</sup> the macrocycle component is also functionalised with an internally directed

pyridyl group: this motif will endotopically bind the copper(I) catalyst during the CuAAC axle-forming reaction, thereby directing the formation of the axle through the cavity of the macrocycle.

The [2]rotaxane **4** was prepared as outlined in Scheme 2. The synthesis of the isophthalamide- and pyridyl-functionalised macrocycle and indolocarbazole thread precursor components **1** and **2** is described in the supporting information. Macrocycle **1** was stirred with 1 equivalent of  $\text{Cu}(\text{CH}_3\text{CN})_4\text{PF}_6$ , 3 equivalents of the bis-azide-terminated threading compound **2** and 6 equivalents of the alkyne functionalised stoppering compound **3**<sup>25</sup> in  $\text{CH}_2\text{Cl}_2$  for 48 hours. After de-metallation ( $\text{EDTA}/\text{NH}_4\text{OH}_{(\text{aq})}$ ), analysis of the crude product distribution using  $^1\text{H}$  NMR spectroscopy indicated approximately 70% conversion of the macrocycle **1** to the interlocked [2]rotaxane **4**, which was isolated in 52% yield after purification by preparative thin layer chromatography.



**Scheme 1.** Design and active metal template based approach to the synthesis of the target indolocarbazole containing [2]rotaxane anion host system.



**Scheme 2.** Active metal template synthesis of the indolocarbazole-containing [2]rotaxane **4**

$^1\text{H}$  NMR techniques were employed to probe the rotaxane's interlocked co-conformation in solution. The  $^1\text{H}$  NMR spectrum of the [2]rotaxane **4** in  $\text{CDCl}_3$  is compared to those of its constituent axle and macrocycle components in Figure 1. A pronounced upfield shift and splitting of the macrocycle hydroquinone proton resonances (6 and 7) is observed upon incorporation of the macrocycle into the [2]rotaxane ( $\Delta\delta = 0.14\text{--}24$  ppm), suggesting that these protons may be shielded by the aromatic ring currents of the axle indolocarbazole group. Further evidence that the macrocycle hydroquinone groups lie in close proximity to the axle indolocarbazole groups in the [2]rotaxane was provided by 2-D ROESY spectroscopy (Figure 2), which indicated through-space ROE interactions between protons 6 and 7 and the indolocarbazole aromatic protons a and b. Since parallel face-centred aromatic stacking interactions between the indolocarbazole and hydroquinone groups, which are both electron-rich, are not predicted to be energetically favourable,<sup>36,37</sup> it is possible that this co-conformation is stabilised by a complementary hydrogen-bonding arrangement, as depicted in Scheme 2, with the indolocarbazole and hydroquinone aromatic systems favouring a parallel offset or perpendicular stacking arrangement. This is supported by the observation that the axle indolocarbazole NH and macrocycle internal isophthalamide proton signals (e, 10

and 11) shift downfield upon rotaxane formation, consistent with hydrogen-bond-induced polarisation of the X—H (X = C, N) bonds (Figure 1).†

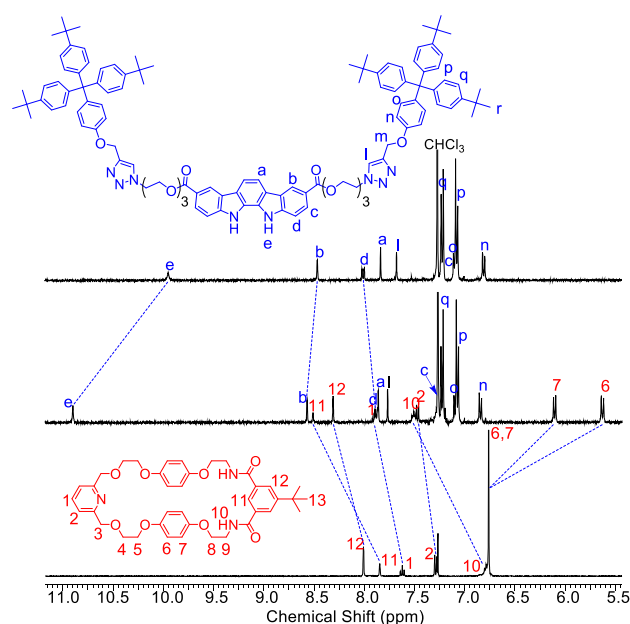


**Figure 1.** Stacked partial  $^1\text{H}$  NMR spectra of the axle **S8** (top), [2]rotaxane **4** (middle) and macrocycle **1** (bottom) in  $\text{CDCl}_3$  at 298 K.

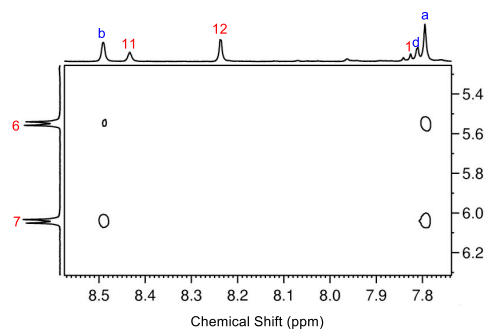


**Figure 2.** Section of the  $^1\text{H}$ - $^1\text{H}$  ROESY NMR spectrum of the [2]rotaxane **4** (500 MHz;  $\text{CDCl}_3$ ; 298 K) showing ROE correlations between the macrocycle hydroquinone and axle indolocarbazole proton resonances.

### Anion binding investigations

**$^1\text{H}$  NMR titration experiments.** The anion binding properties of the [2]rotaxane **4** were probed using  $^1\text{H}$  NMR titration experiments in an organic-aqueous acetone- $\text{d}_6$ : $\text{D}_2\text{O}$  95:5 solvent mixture. Prior to this analogous titration experiments were performed using the indolocarbazole thread **2** and macrocycle **1** in order to provide preliminary insight into the anion binding capabilities of the individual axle indolocarbazole and macrocycle isophthalamide sub-components which comprise the rotaxane's interlocked binding cavity. However, upon addition of increasing concentrations of the tetrabutylammonium (TBA) salts of a range of anions to a solution of the macrocycle **1** in acetone- $\text{d}_6$ : $\text{D}_2\text{O}$  95:5 minimal perturbations of the proton shifts were observed, suggesting that the macrocycle's bis-amide hydrogen-bonding cleft does not interact with the anions to a significant degree in the competitive acetone/ $\text{D}_2\text{O}$  solvent medium.

In contrast for the more potent indolocarbazole receptor **2** clear  $^1\text{H}$  NMR evidence of anion recognition was obtained. Although the indolocarbazole NH resonances are not observed in this protic solvent medium owing to hydrogen-deuterium exchange, complexation could be inferred from the observed downfield perturbations in the aromatic CH proton environment d (Figure S16, ESI). Association constants were determined by non-linear least squares analysis of the anion-induced changes in the chemical shift of proton d using WinEQNMR<sup>38</sup> software (Table 1 and Figure S17, ESI). Compound **2** was found to bind the monoanions in a 1:1 stoichiometric ratio with moderate affinities. The observed order of selectivity ( $\text{AcO}^- > \text{F}^- > \text{H}_2\text{PO}_4^- > \text{Cl}^- > \text{Br}^- > \text{NO}_3^-$ ) is generally consistent with the anion recognition behaviour of previously reported acyclic indolocarbazole anion receptors<sup>8,39–43</sup> and broadly correlates with the relative basicities of the monoanions. The marked preference for acetate may additionally reflect optimal geometric complementarity between the Y-shaped carboxylate anion and the spatial arrangement of the indolocarbazole motif's two preorganised NH hydrogen-bond-donor groups.

Similarly, addition of anions as their TBA salts to the [2]rotaxane **4** in acetone- $\text{d}_6$ : $\text{D}_2\text{O}$  95:5 led to progressive shifts in a number of the axle and macrocycle proton environments, indicative of the fast exchange complexation of the anion guests by the [2]rotaxane host molecule (Figure 3). Upfield

perturbations in the internal macrocycle proton 11 and, in most cases, the indolocarbazole aromatic proton d imply that both the axle indolocarbazole and macrocycle isophthalamide groups participate in  $\text{C}-\text{H}\cdots\text{X}^-$  as well as  $\text{N}-\text{H}\cdots\text{X}^-$  hydrogen bonding interactions with the encapsulated anion. The macrocycle hydroquinone proton signals 6 and 7 shift upfield upon anion addition, suggesting that the anion-induced co-conformational changes lead to increased overlap between the  $\pi$  electron clouds of the macrocycle hydroquinone and indolocarbazole functional groups.

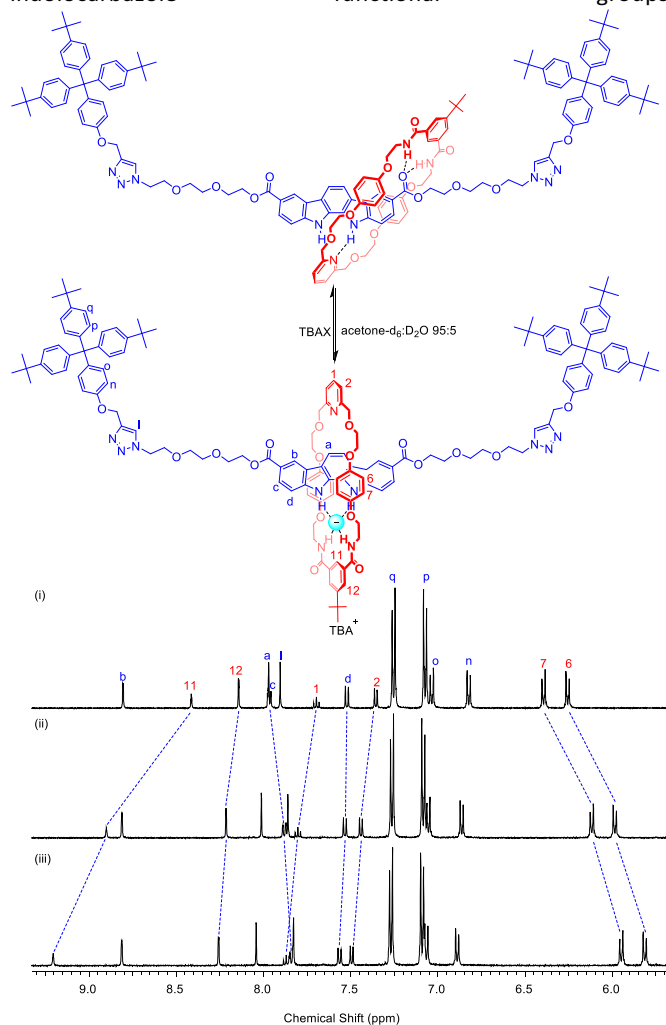


**Figure 3.**  $^1\text{H}$  NMR spectra of a 1.5 mM solution of the [2]rotaxane **4** in acetone- $\text{d}_6$ : $\text{D}_2\text{O}$  95:5 (500 MHz; 298 K) in the presence of (i) 0, (ii) 1 and (iii) 5 equivalents of  $\text{TBA}\cdot\text{H}_2\text{PO}_4$ .

Association constants for 1:1 stoichiometric binding were determined by WinEQNMR<sup>38</sup> analysis of the titration data, monitoring the chemical shift changes of the internal macrocycle isophthalamide proton 11 (Table 1 and Figure S17, ESI). The [2]rotaxane displays a higher affinity for all of the monoanions studied compared to the individual macrocycle and axle components, which can be attributed to the availability of convergent hydrogen-bond-donor groups from both the axle indolocarbazole and macrocycle isophthalamide groups in the multivalent [2]rotaxane host system. The anion selectivity trend observed for the [2]rotaxane **4** generally mirrors that of the indolocarbazole receptor **2**. However, while the rotaxane retains a marginal overall preference for acetate,

the most dramatic enhancement is for the dihydrogenphosphate anion, which intimates that the topological arrangement of the hydrogen bond donor groups in the rotaxane's interlocked binding cavity most effectively complements the tetrahedral geometry of the dihydrogenphosphate anion.

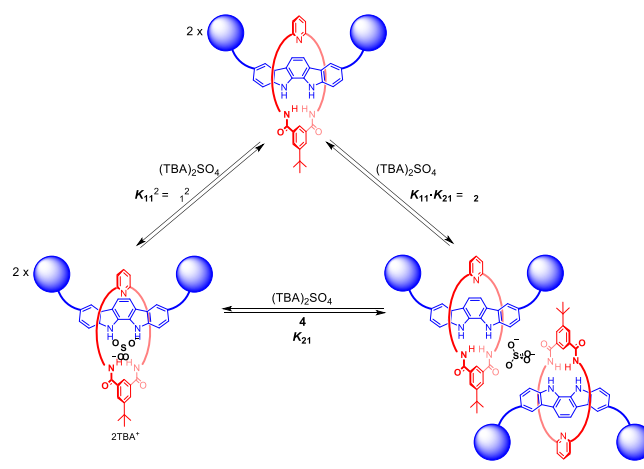
**Table 1.** Association constants for 1:1 complexes of the [2]rotaxane **4** with various anions in acetone- $d_6$ : $D_2O$  95:5 at 298 K.

Anion <sup>b</sup>	$K (M^{-1})^a$	
	<b>2</b>	<b>4</b>
F <sup>-</sup>	378 (15)	739 (39)
Cl <sup>-</sup>	200 (8)	516 (11)
Br <sup>-</sup>	107 (1)	142 (2)
AcO <sup>-</sup>	1347 (40)	2359 (129)
H <sub>2</sub> PO <sub>4</sub> <sup>-</sup>	286 (8)	2049 (127)
NO <sub>3</sub> <sup>-</sup>		

<sup>a</sup>Association constant calculated by analysis of the anion induced changes in the chemical shift of proton 11 using WinEQNMR<sup>38</sup> software. Estimated expanded uncertainties at the 95% confidence interval level are given in parentheses. <sup>b</sup>All anions added as TBA salts. <sup>c</sup>Chemical shift changes too small to allow for accurate binding constant determination over the anion concentration range covered.

**Sulfate binding experiments.** The apparent complementarity between the [2]rotaxane's interlocked binding cavity and the dihydrogenphosphate anion encouraged us to also investigate the rotaxane's binding affinity for the tetrahedral sulfate dianion, since a number of literature reports have established a precedent for strong and selective sulfate anion binding by indolocarbazole-containing receptors.<sup>14,17,21</sup> Upon titration of (TBA)<sub>2</sub>SO<sub>4</sub> into a solution of the [2]rotaxane **4** in acetone- $d_6$ : $D_2O$  95:5 the <sup>1</sup>H NMR chemical shifts of several of the rotaxane proton environments exhibited complex sulfate concentration dependencies, indicating a composite binding mode. For example, the binding curves obtained by following the indolocarbazole aromatic protons c and d display sharp minima after addition of approximately 0.5 molar equivalents of the sulfate dianion (Figure 4), while a slight sigmoidal feature in the titration curve for the macrocycle internal isophthalamide proton 11 can also be discerned at low sulfate concentration. This is consistent with the initial formation of a 2:1 stoichiometric **4**:SO<sub>4</sub><sup>2-</sup> complex which is replaced by a 1:1 stoichiometric complex at higher sulfate concentration (Scheme 4). The 2:1 **4**:SO<sub>4</sub><sup>2-</sup> complex is presumed to be a sandwich-type assembly in which the sulfate anion nests within an enclosed cavity formed by the close approach of two rotaxane molecules, which allows the anion to participate in a maximum of eight N-H—O hydrogen-bonding interactions (Scheme 3). There are a number of literature precedents for the formation of similar 2:1 receptor:SO<sub>4</sub><sup>2-</sup> complexes.<sup>21,44–46</sup> The formation of these higher order aggregates is conceivably driven by the dianion's strong hydrogen-bond-acceptor character and preference for high coordination numbers of up to 12.<sup>47</sup> Analysis of the titration data using WinEQNMR<sup>38</sup> software, monitoring the internal macrocycle 11, determined overall equilibrium constants of  $\beta_2 = 216315 (33950) M^{-2}$  and  $\beta_1 = 4518 (872) M^{-1}$  for formation of the 2:1 and 1:1 receptor:anion complexes respectively (Table 2). Pleasingly good numerical agreement with these values was observed

when the equilibrium constants were determined based on the chemical shift changes of protons a and c (Table S1, ESI and Figure 4).



**Scheme 3.** Equilibria between the free [2]rotaxane **4** and 2:1 and 1:1 stoichiometric **4**:SO<sub>4</sub><sup>2-</sup> complexes observed on titration of (TBA)<sub>2</sub>SO<sub>4</sub> into acetone- $d_6$ : $D_2O$  solutions of the [2]rotaxane.

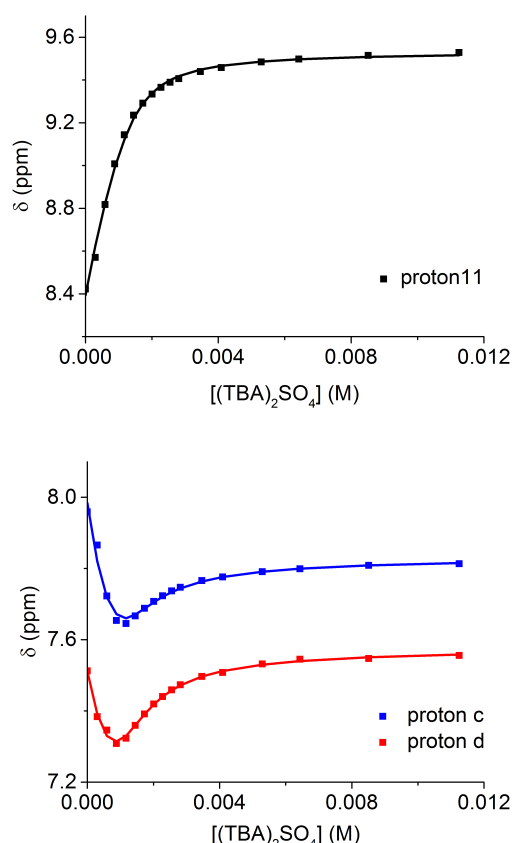


**Figure 4.** Changes in the <sup>1</sup>H NMR chemical shifts of protons 11, c and d as a function of [(TBA)<sub>2</sub>SO<sub>4</sub>] observed during titration of (TBA)<sub>2</sub>SO<sub>4</sub> into an acetone- $d_6$ : $D_2O$  95:5 solution of the [2]rotaxane **4** at 298 K. Square points represent experimental data; continuous lines represent theoretical binding curves for the calculated equilibrium constant values shown in Tables 2 and S1 (ESI). For proton assignments, see Figures 1 and 3.

When the titration experiment was repeated in the more competitive solvent mixture acetone- $d_6$ : $D_2O$  90:10 the

calculated values of  $\beta_2$  and  $\beta_1$  were both found to be suppressed (Table 2 and Figure S18, ESI). However, it is notable that while the  $K_{11}$  ( $\beta_1$ ) equilibrium is appreciably disfavoured in the presence of a higher percentage of D<sub>2</sub>O, the change in the  $K_{21}$  equilibrium constant is comparatively insignificant. This may reflect a greater solvophobic contribution to the  $K_{21}$  equilibrium process.

**Table 2.** Association constants for 2:1 and 1:1 complexes of the [2]rotaxane **4** with  $\text{SO}_4^{2-}$  anions in acetone- $\text{d}_6$ :D<sub>2</sub>O 95:5 and acetone- $\text{d}_6$ :D<sub>2</sub>O 90:10 at 298 K.<sup>a</sup>

Solvent	acetone- $\text{d}_6$ :D <sub>2</sub> O 95:5 <sup>b</sup>	acetone- $\text{d}_6$ :D <sub>2</sub> O 90:10 <sup>c</sup>
$K_{11} = \beta_1$ ( $\text{M}^{-1}$ )	4518 (872)	280 (17)
$K_{21}$ ( $\text{M}^{-1}$ )	48 (12)	94 (11)
$K_{11} \cdot K_{21} = \beta_2$ ( $\text{M}^{-2}$ )	216315 (33950)	26366 (2713)

<sup>a</sup> $\text{SO}_4^{2-}$  added as a TBA salt. <sup>b</sup>Association constants calculated by analysis of the changes in the chemical shift of proton 11 using WinEQNMR<sup>38</sup> software. Estimated expanded curve-fitting uncertainties at the 95% confidence interval level are given in parentheses. <sup>c</sup>Association constants calculated by analysis of the changes in the chemical shift of proton c using WinEQNMR<sup>38</sup> software.

**Fluorescence anion titration experiments.** Taking advantage of the axle-integrated indolocarbazole fluorophore, fluorescence titration experiments were undertaken to probe the [2]rotaxane's anion sensing capabilities. The emission spectrum of the [2]rotaxane **4** in acetone:H<sub>2</sub>O 95:5 shows a broad, featureless emission band with a maximum at 410 nm ( $\lambda_{\text{ex}} = 333$  nm). Addition of the TBA salts of  $\text{AcO}^-$ ,  $\text{H}_2\text{PO}_4^-$ ,  $\text{F}^-$ ,  $\text{Cl}^-$  and  $\text{SO}_4^{2-}$  led to substantial (15–40 nm) bathochromic shifts in the maximum of the emission band, along with significant quenching ( $\text{F}^-$ ,  $\text{AcO}^-$ ) or enhancements ( $\text{Cl}^-$ ) of the emission intensity in some cases (Figure 5a and Figures S19a-f, ESI). For  $\text{Br}^-$  and  $\text{NO}_3^-$  anions comparatively minor spectral changes were observed, consistent with the  $^1\text{H}$  NMR evidence for weak interactions between these guest anions and the rotaxane host. For the monoanions, association constants for 1:1 stoichiometric binding were determined by global analysis of the fluorescence titration data using Specfit<sup>48</sup> software (Table 3, Figure 5b), and are in good overall agreement with the  $^1\text{H}$  NMR-derived binding data.<sup>¶</sup>

**Table 3.** Association constants,  $\log K$  and  $K$  ( $\text{M}^{-1}$ ), for 1:1 complexes of the [2]rotaxane **4** with various anions in acetone:H<sub>2</sub>O 95:5 at 298 K and observed change in the maximum wavelength of the emission band,  $\Delta\lambda_{\text{max(em)}}$  (nm), in the presence of each anion.

Anion <sup>b</sup>	$\log K^a$	$K(\text{M}^{-1})$	$\Delta\lambda_{\text{max(em)}}(\text{nm})^c$
$\text{F}^-$	3.12 (0.01)	1322	+ 40
$\text{Cl}^-$	2.76 (0.02)	573	+ 15
$\text{Br}^-$	1.65 (0.07)	45	+ 10
$\text{AcO}^-$	3.32 (0.01)	2103	+ 35
$\text{H}_2\text{PO}_4^-$	3.44 (0.04)	2728	+ 40
$\text{NO}_3^-$	1.47 (0.05)	29	+ < 5

<sup>a</sup> $\log K$  values calculated by analysis of the anion induced changes in the fluorescence emission band of the [2]rotaxane **4** using Specfit<sup>48</sup> software. Estimated standard deviations are given in parentheses. <sup>b</sup>All anions added as TBA salts. <sup>c</sup> $\Delta\lambda_{\text{max(em)}}$  value are quoted to the nearest 5 nm.  $\lambda_{\text{ex}} = 333$  nm. Final anion concentrations: 9.6–10.0 mM.

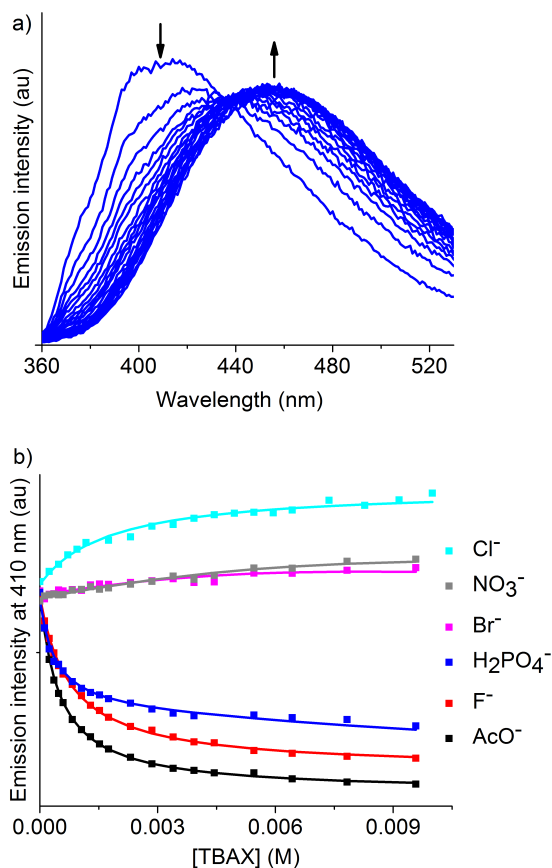


**Figure 5.** a) Changes in the fluorescence emission spectrum of a 15  $\mu\text{M}$  solution of the [2]rotaxane **4** in acetone:H<sub>2</sub>O 95:5 on addition of an increasing concentration of  $\text{TBAH}_2\text{PO}_4$ . b) Changes in the emission intensity at 410 nm as a function of [TBAX] on addition of various monoanions as their TBA salts. Square points represent experimental data; continuous lines represent theoretical binding curves for the equilibrium constant values displayed in Table 3. Temperature: 298 K.  $\lambda_{\text{ex}} = 333$  nm.

## Conclusions

An active metal template strategy was used to synthesise a neutral [2]rotaxane anion host system containing an indolocarbazole-based axle component and an isophthalamide-functionalised macrocycle component.  $^1\text{H}$  NMR titrations experiments demonstrated that the [2]rotaxane binds a range of halide and oxoanions with higher affinities than its constituent non-interlocked axle and macrocycle components in acetone- $\text{d}_6$ :D<sub>2</sub>O 95:5, with, importantly, an unusual and rare preference for acetate and dihydrogenphosphate over halides among the monoanions. The [2]rotaxane displays an overall selectivity for the divalent sulfate anion, forming a 2:1 receptor: $\text{SO}_4^{2-}$  complex at low sulfate concentrations which is replaced by a 1:1 complex at higher sulfate concentrations. Fluorescence spectroscopic anion titrations experiments indicated that the [2]rotaxane host system is also able to sense anions via significant changes in the maximum wavelength and intensity of its emission spectrum.



## Acknowledgements

We thank the European Research Council for funding under the European Union's 7<sup>th</sup> Framework programme (FP7/2007–2013), ERC advanced grant agreement number 267426 and the Engineering and Physical Sciences Research Council for a post-doctoral fellowship (KMM).

## Notes and references

‡ As further evidence for the existence of the proposed stabilising complementary hydrogen bonding arrangement, spontaneous pseudorotaxane assembly was observed on addition of the indolocarbazole threading compound **2** to a solution of macrocycle **1** in CDCl<sub>3</sub> at 298 K, evidenced by diagnostic upfield shifts in the macrocycle hydroquinone proton <sup>1</sup>H NMR resonances. Both Cl<sup>−</sup> anions and Cu(I) cations, which are expected to compete with the indolocarbazole threading compound for binding to the macrocycle's isophthalamide and pyridyl sub-units respectively, were qualitatively observed to destabilise the pseudorotaxane assembly.

§ The non-interlocked axle component (compound **S8**, ESI) of the [2]rotaxane **4** was isolated as a side-product of the [2]rotaxane synthesis reaction.

¶ Interestingly, with one exception,<sup>14</sup> such substantial anion-induced red shifts in the emission spectrum have not previously been observed for indolocarbazole-based anion receptors.<sup>8,17,19,43,49</sup> We are continuing to investigate the cause of the anion-induced fluorescence responses.

¶ Global analysis of the data for the (TBA)<sub>2</sub>SO<sub>4</sub> fluorescence titration experiment again suggested the operation of 2:1 and 1:1 stoichiometric host:guest equilibrium binding processes but we were unable to determine quantitative binding constants within reasonable error from this experiment.

- 1 The Nobel Prize in Chemistry 2016 - Advanced Information, [https://www.nobelprize.org/nobel\\_prizes/chemistry/laureates/2016/advanced.html](https://www.nobelprize.org/nobel_prizes/chemistry/laureates/2016/advanced.html).
- 2 D. A. Leigh, *Angew. Chem. Int. Ed.*, 2016, **55**, 14506–14508.
- 3 S. Erbas-Cakmak, D. A. Leigh, C. T. McTernan and A. L. Nussbaumer, *Chem. Rev.*, 2015, **115**, 10081–10206.
- 4 C. O. Dietrich-Buchecker, J. P. Sauvage and J. P. Kintzinger, *Tetrahedron Lett.*, 1983, **24**, 5095–5098.
- 5 C. O. Dietrich-Buchecker, J. P. Sauvage and J. M. Kern, *J. Am. Chem. Soc.*, 1984, **106**, 3043–3045.
- 6 G. T. Spence and P. D. Beer, *Acc. Chem. Res.*, 2013, **46**, 571–586.
- 7 A. Caballero, F. Zapata and P. D. Beer, *Coord. Chem. Rev.*, 2013, **257**, 2434–2455.
- 8 D. Curiel, A. Cowley and P. D. Beer, *Chem. Commun.*, 2005, 236–238.
- 9 K.-J. Chang, D. Moon, M. S. Lah and K.-S. Jeong, *Angew. Chem. Int. Ed.*, 2005, **44**, 7926–7929.
- 10 N.-K. Kim, K.-J. Chang, D. Moon, M. S. Lah and K.-S. Jeong, *Chem. Commun.*, 2007, 3401–3403.
- 11 Y. Zhao, Y. Li, Y. Li, C. Huang, H. Liu, S.-W. Lai, C.-M. Che and D. Zhu, *Org. Biomol. Chem.*, 2010, **8**, 3923–3927.
- 12 C.-H. Lee, H. Yoon, P. Kim, S. Cho, D. Kim and W.-D. Jang, *Chem. Commun.*, 2011, **47**, 4246–4248.
- 13 J. Suk and K.-S. Jeong, *J. Am. Chem. Soc.*, 2008, **130**, 11868–11869.
- 14 J. Kim, H. Juwarker, X. Liu, M. S. Lah and K.-S. Jeong, *Chem. Commun.*, 2010, **46**, 764–766.
- 15 J. Suk, J. Kim and K.-S. Jeong, *Chem. – Asian J.*, 2011, **6**, 1992–1995.
- 16 J. Suk, D. A. Kim and K.-S. Jeong, *Org. Lett.*, 2012, **14**, 5018–5021.
- 17 H. J. Kim, J.-M. Suk and K.-S. Jeong, *Supramol. Chem.*, 2013, **25**, 46–53.
- 18 D. A. Kim, P. Kang, M.-G. Choi and K.-S. Jeong, *Chem. Commun.*, 2013, **49**, 9743–9745.
- 19 M. K. Chae, J. Suk and K.-S. Jeong, *Tetrahedron Lett.*, 2010, **51**, 4240–4242.
- 20 Y. Zhao, Y. Li, Y. Li, H. Zheng, X. Yin and H. Liu, *Chem. Commun.*, 2010, **46**, 5698–5700.
- 21 M. J. Chmielewski, L. Zhao, A. Brown, D. Curiel, M. R. Sambrook, A. L. Thompson, S. M. Santos, V. Felix, J. J. Davis and P. D. Beer, *Chem. Commun.*, 2008, 3154–3156.
- 22 However, sulfate and fluoride anion templation was successfully applied to the assembly of a [2] rotaxane comprising indolocarbazole axle and isophthalamide macrocycle components on a gold surface: L. Zhao, J. J. Davis, K. M. Mullen, M. J. Chmielewski, R. M. J. Jacobs, A. Brown and P. D. Beer, *Langmuir*, 2009, **25**, 2935–2940.
- 23 A. Brown, K. M. Mullen, J. Ryu, M. J. Chmielewski, S. M. Santos, V. Felix, A. L. Thompson, J. E. Warren, S. I. Pascu and P. D. Beer, *J. Am. Chem. Soc.*, 2009, **131**, 4937–4952.
- 24 For a review of early work on the active metal template synthesis of rotaxane and catenane molecules, see: J. D. Crowley, S. M. Goldup, A.-L. Lee, D. A. Leigh and R. T. McBurney, *Chem. Soc. Rev.*, 2009, **38**, 1530–1541.
- 25 V. Aucagne, K. D. Hänni, D. A. Leigh, P. J. Lusby and D. B. Walker, *J. Am. Chem. Soc.*, 2006, **128**, 2186–2187.
- 26 V. Aucagne, J. Berná, J. D. Crowley, S. M. Goldup, K. D. Hänni, D. A. Leigh, P. J. Lusby, V. E. Ronaldson, A. M. Z. Slawin, A. Viterisi and D. B. Walker, *J. Am. Chem. Soc.*, 2007, **129**, 11950–11963.
- 27 S. M. Goldup, D. A. Leigh, T. Long, P. R. McGonigal, M. D. Symes and J. Wu, *J. Am. Chem. Soc.*, 2009, **131**, 15924–15929.
- 28 P. E. Barran, H. L. Cole, S. M. Goldup, D. A. Leigh, P. R. McGonigal, M. D. Symes, J. Wu and M. Zengerle, *Angew. Chem. Int. Ed.*, 2011, **50**, 12280–12284.
- 29 M. J. Langton, J. D. Matichak, A. L. Thompson and H. L. Anderson, *Chem. Sci.*, 2011, **2**, 1897.
- 30 B. Lewandowski, G. De Bo, J. W. Ward, M. Papmeyer, S. Kuschel, M. J. Aldegunde, P. M. E. Gramlich, D. Heckmann, S. M. Goldup, D. M. D'Souza, A. E. Fernandes and D. A. Leigh, *Science*, 2013, **339**, 189–193.
- 31 A. Noor, S. C. Moratti and J. D. Crowley, *Chem Sci*, 2014, **5**, 4283–4290.
- 32 E. A. Neal and S. M. Goldup, *Chem. Sci.*, 2015, **6**, 2398–2404.
- 33 J. E. M. Lewis, J. Winn, L. Cera and S. M. Goldup, *J. Am. Chem. Soc.*, 2016, **138**, 16329–16336.
- 34 J. Y. C. Lim, I. Marques, A. L. Thompson, K. E. Christensen, V. Félix and P. D. Beer, *J. Am. Chem. Soc.*, 2017, **139**, 3122–3133.
- 35 For a rare previously reported example of an oxoanion selective [2]rotaxane host system, see: S. P. Cornes, C. H. Davies, D. Blyghton, M. R. Sambrook and P. D. Beer, *Org. Biomol. Chem.*, 2015, **13**, 2582–2587.
- 36 C. A. Hunter and J. K. M. Sanders, *J. Am. Chem. Soc.*, 1990, **112**, 5525–5534.
- 37 C. R. Martinez and B. L. Iverson, *Chem. Sci.*, 2012, **3**, 2191–2201.
- 38 M. J. Hynes, *J. Chem. Soc., Dalton Trans.*, 1993, 311–312.

- 39 K.-J. Chang, M. K. Chae, C. Lee, J.-Y. Lee and K.-S. Jeong, *Tetrahedron Lett.*, 2006, **47**, 6385–6388.
- 40 T. H. Kwon and K.-S. Jeong, *Tetrahedron Lett.*, 2006, **47**, 8539–8541.
- 41 J. Ju, M. Park, J. Suk, M. S. Lah and K.-S. Jeong, *Chem. Commun.*, 2008, 3546–3548.
- 42 T. Wang, H.-F. Wang and X.-P. Yan, *CrystEngComm*, 2010, **12**, 3177–3182.
- 43 G. Sánchez, D. Curiel, A. Tárraga and P. Molina, *Sensors*, 2014, **14**, 14038–14049.
- 44 S. Kubik, R. Goddard, R. Kirchner, D. Nolting and J. Seidel, *Angew. Chem. Int. Ed.*, 2001, **40**, 2648–2651.
- 45 M. A. Hossain, J. M. Llinares, D. Powell and K. Bowman-James, *Inorg. Chem.*, 2001, **40**, 2936–2937.
- 46 K. M. Bąk and M. J. Chmielewski, *Chem Commun*, 2014, **50**, 1305–1308.
- 47 L. Chertanova and C. Pascard, *Acta Crystallogr. B*, 1996, **52**, 677–684.
- 48 F. D. Barb, O. Netoiu, M. Sorescu and M. Weiss, *Comput. Phys. Commun.*, 1992, **69**, 182–186.
- 49 T. Wang, Y. Bai, L. Ma and X.-P. Yan, *Org. Biomol. Chem.*, 2008, **6**, 1751.